inter.noise
HAMBURG 2016

Low frequency sound energy decay in coupled volume rooms: results from a numerical study

Tim TIJSMA[1]; Maarten HORNIKX[1]

[1] Eindhoven University of Technology, The Netherlands

ABSTRACT

In performance spaces, double sloped sound energy decays can be created intentionally to combine the two contradicting qualities clarity and reverberance. However, in office environments with atria, unintentional occurrence of double sloped decays might lead to noise nuisance. This research focuses on the low frequency range. In contrast to the high frequency range, the double slope effect is expected to be frequency dependent for low frequencies. The sound field is simulated using the finite element method by solving the acoustic wave equation, for two rectangular rooms with varying location and distribution of apertures in the partition wall. The results show a varying decay curve over different positions in the less reverberant room, independent of the aperture location and distribution. The location of the apertures shows to have a large influence on the decay curve due to the modal shapes in the secondary room. A systematic frequency dependence of the decay curve has not been found, which would be present due to reduced aperture transparency at low frequencies. It is expected to be more distinctly present in larger volume room systems. Finally, the use of quantifiers to identify double sloped decay curves is discussed.

Keywords: coupled volume rooms, low frequency sound, non-exponential decays, double slope effect
I-INCE Classification of Subjects Number(s): 25.4

1. INTRODUCTION

When two rooms are connected by an aperture, they form a system of acoustically coupled volume rooms. An important property of such a room system is that sound energy does not necessarily decay at an exponential rate, meaning that the decay is split in two stages, the early and the late decay. In both stages the sound energy decays at a different (exponential) rate. This non-exponential (double sloped) decay can be an appreciated acoustic quality at one hand but can also be the cause of noise nuisance at the other.

Clarity and reverberance are two qualities sought after in performance spaces such as concert halls. Normally these are contradicting qualities since clarity is achieved through a fast initial decay and reverberance is characterized by slow decay. In coupled volume rooms the two can coexist since a concave double sloped decay can have both a fast initial decay in the first stage and a long overall decay due to the more shallow slope of second stage of the decay curve. When a coupled volume room system is created unintentionally, for example in an office environment where a room is coupled to an atrium, a double sloped decay can cause nuisance. When using traditional statistical acoustics methods such as the Sabine, Eyring or Millington Sette model for predicting reverberation time in the design stage of spaces, the effects of the second volume are not taken into account in the prediction (1–3). This can lead to a severe underestimation of the reverberation.

Previous research has been conducted mainly using frequency independent methods such as geometrical- and energy based acoustics methods (4–8). These methods either assume a diffuse sound field or represent waves by rays, excluding some wave effects. For low frequencies, the sound field is far from diffuse and phase effects become stronger (9). To gain an insight in the decay behavior of coupled volume rooms at low frequencies, simulations are performed using a numerical method that solves the wave equation.

[1] t.w.tijsma@student.tue.nl

2. BACKGROUND

2.1 Criteria for the occurrence of the double slope effect

In coupled volume rooms, energy transfer takes place between two rooms. When a sound source is located in the primary room, the sound incident on the aperture surface is transferred to the secondary room. Reflections in the secondary room incident on the aperture surface are in turn transferred back to the primary room with a certain delay (10). The delayed feedback of energy can become predominant in the sound field of the primary room, causing the second stage of the decay with a slower decay rate. In this case, the decay curve of the primary room is double sloped.

With regards to room geometry and surface materials, the occurrence and magnitude of the double slope effect is mainly depending on two factors: reverberation and aperture size (10).

As regards reverberation, the secondary room has to be sufficiently reverberant for the delayed feedback to become predominant over the remaining sound field. This can be expressed in the dimensionless parameter RT ratio (reverberation time ratio), calculated by dividing the reverberation time of the secondary room by the reverberation time of the primary room. Typically, the RT ratio should be at least 3.5 but preferably more than 5 (4,8,11,12).

As regards the aperture size, the different rooms in the system are coupled by means of an aperture that allows an exchange of energy. When the aperture is very large, the coupling is strong and the rooms are connected as if they are one. When the aperture is very small the coupling is weak and the room system is separated into two individual systems. For a double sloped decay to occur as an effect of the coupled volumes, the rooms have to be loosely coupled (13). The total area of the apertures can be quantified as aperture opening, defined as the percentage of the opening from the total available boundary surface area of the primary room excluding the floor area. This yields a normalised quantity that can be compared for different primary rooms (14). The optimal aperture opening to obtain a double sloped decay is found between 0.5% and 1.5% of the available surface area in the primary room (11,15,16). From 5.0% aperture opening the decay profile is only slightly double sloped, approaching an exponential decay for a single combined room (14,17).

Apertures become acoustically less transparent with decreasing frequency (9). To approximate the acoustic transparency of the apertures for different aperture dimensions, the apertures are treated as a radiating piston in a plane boundary (9). This is represented by equation 1, which describes the radiated power of a piston with uniform velocity amplitude in Watt.

$$P_r = \frac{1}{2}\hat{v}_0^2 S Z_0 \left(1 - \frac{2\boldsymbol{J}_1(2ka)}{2ka}\right) \tag{1}$$

Where $\hat{v}_0$ [m/s] is the mean particle velocity at the surface, Z_0 [Pa·s/m] is the impedance of air, $\boldsymbol{J}_1$ is the Bessel function of the first order, k [m^{-1}] is the wave number and a [m] is the radius of the piston (The square apertures are represented by a circle with a radius that results in an equal surface area as the aperture.)

2.2 Computational model

The finite element method (FEM) is used to solve the wave equation, making use of the acoustics module of the COMSOL multiphysics software environment, version 5.0. The walls are represented by impedance boundary conditions.

An omnidirectional source is represented by a 0.01 m radius sphere with a pressure boundary following a pressure profile in time described by the derivative of a Gaussian pulse. Because of the limited pulse width in the frequency domain, two separate simulations are performed with a different pulse duration; the results for the 31.5 Hz and 63 Hz octave are extracted from a simulation with longer pulse duration than the results for the 125 Hz octave.

Additionally, a statistical method is used for comparative purposes in analysing the frequency dependency of the double slope effect. The model is given in equation 2 and equation 3 and treats the coupled volumes as a system of sub rooms that only interact through exchange of energy between the two different sound fields through the aperture(s). The energy density for the primary (P) and secondary (S) room is calculated using equation 2 and equation 3 (7).

$$E_P(t) = E_{P1}\exp(-2\delta_I t) + E_{S2}\frac{k_P}{1-\delta_{II}/\delta_P}exp(-2\delta_{II}t) \quad (2)$$

$$\mathrm{E_S(t)} = \mathrm{E_{P1}}\frac{\mathrm{k_P}}{1-\delta_\mathrm{I}/\delta_\mathrm{S}}\exp(-2\delta_\mathrm{I}\mathrm{t}) + \mathrm{E_{S2}}\exp(-2\delta_\mathrm{II}\mathrm{t}) \quad (3)$$

Where E_{P1} and E_{S2} are the initial values of the decay, k_P [-] is the coupling strength of the primary room and δ_I [-] and δ_{II} [-] are the eigenfactors of the coupled rooms

2.3 Quantifiers for double sloped decays

Several quantifiers have been suggested and evaluated to quantify the double slope effect (4,12,14,18). Among these quantifiers are the coupling coefficient (T_{30}/T_{15}), coupling constant (T_{60}/T_{15}), LDT/EDT and LDT/T_{10} that relate the decay time of the early decay to the overall decay time or to the decay time determined over the late decay. The decay times are determined over two fixed ranges within the sound energy decay where it is assumed that this range solely contains a single stage of the decay. In practice these ranges often contain a part of the transition between the two stages, resulting in misrepresentation of the results (19). Additionally, the quantifiers do not uniquely describe a double sloped decay, meaning that different decay curves could have the same quantifier value.

To overcome these limitations, in various studies the combination of the two quantifiers decay ratio and ΔdB (ΔL) is used (4,14). The decay ratio relates the slope of the early decay to the slope of the late decay. Instead of evaluating a fixed range, both parts of the decay are extrapolated as shown by the dotted lines in figure 1. The quotient of the two slopes is the decay ratio. ΔdB is defined as the *y* intercept (at t = 0 s) of the extrapolated late decay, this is elucidated in figure 1. Also for this combination of quantifiers additional information is needed to uniquely quantify a decay curve. For example the diverging decay curves (the late decays diverge in the evaluation range of 0 dB to -60 dB) in figure 1 both have a decay ratio of 2.5 and ΔdB equal to 20 dB. Another shortcoming of these combined quantifiers while comparing decay curves with diverging late decays is that they fail to give a clear insight in the length of the overall decay.

In this study, the compared decay curves mainly have diverging late decays, leaving the ΔdB and decay ratio unable to make a clear comparison. Therefore, the 90 dB decay time is used as additional parameter, defined as the time to decay from 0 to -90 dB. The authors realise that -90 dB is a very low level that generally lies outside of the audible range. Therefore, the 60 dB decay time would be a better and more generally applicable quantifier. In this study however, the transition to the late decay is sometimes not fully completed within 60 dB decay, thus the use of the 60 dB decay time would misrepresent the results.

The combination of the 60 dB decay time and decay ratio has similar shortcomings as the combination with ΔdB. For example the two different decay curves with converging late decay in figure 1 have an equal decay ratio and equal 60 dB decay time. Therefore the 60 dB decay time should not replace ΔdB but is to be used as an addition. The combination of three quantifiers has the ability to uniquely describe a decay curve.

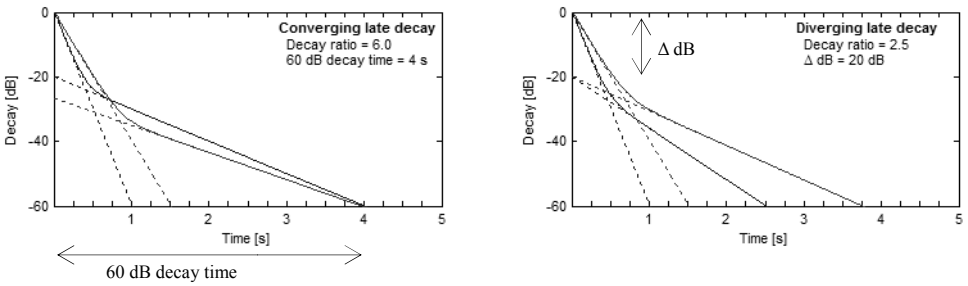

Figure 1 – Example decay curves with left: converging and right: diverging late decays.

3. Computational analysis

3.1 Variant study

This study focuses on frequency dependence and two geometry related parameters, aperture location and aperture distribution, on the double slope effect. The effect of changing these parameters is studied using a simple geometry that consists of two different sized rectangular rooms connected by the coupling surface. The amount of apertures and their location vary in nine configurations with a constant total aperture area of 1.0%, and 1, 2 or 4 equally sized apertures on three different sets of locations. Table 1 shows the configurations denoted by configuration number, corresponding aperture distribution and location of the aperture centre. The location is given on a two dimensional coordinate system projected on the coupling surface of the primary room.

Table 1 – Configurations

#	Ap. size [m²]	Ap. centre 1 (x;y)[m]	Ap. centre 2 (x;y)[m]	Ap. centre 3 (x;y)[m]	Ap. centre 4 (x;y)[m]
1-1	1.25	3.2 ; 2.0	-	-	-
1-2	1.25	2.4 ; 2.5	-	-	-
1-3	1.25	1.6 ; 3.0	-	-	-
2-1	0.62	1.6 ; 2.0	4.8 ; 2.0	-	-
2-2	0.62	1.6 ; 2.5	4.8 ; 1.5	-	-
2-3	0.62	1.6 ; 3.0	1.6 ; 1.0	-	-
3-1	0.31	1.6 ; 3.0	4.8 ; 3.0	1.6 ; 1.0	4.8 ; 1.0
3-2	0.31	2.0; 3.0	5.2 ; 3.0	1.2 ; 1.0	4.4 ; 1.0
3-3	0.31	2.4 ; 3.0	5.6 ; 3.0	0.8 ; 1.0	4.0 ; 1.0

The size (l·w·h = 6.40 m · 5.10 m · 4.0 m) and reverberation time (T_{60} = 0.8 s) of the primary room are similar to a typical office space. The secondary room has a larger size (l·w·h = 7.20 m · 5.80 m · 4.5 m). A floor plan and vertical cross-section are shown in figure 2. The reverberation time (T_{60} = 4.0 s) required to achieve the desired RT ratio of 5 is achieved through wall characteristics rather than sheer size as an attempt to limit the computational demand. The room boundaries have a spatially and spectrally uniform distribution of sound absorption, with a real valued surface impedance of 9000 Pa·s/m for the primary room and 43000 Pa·s/m for the secondary room.

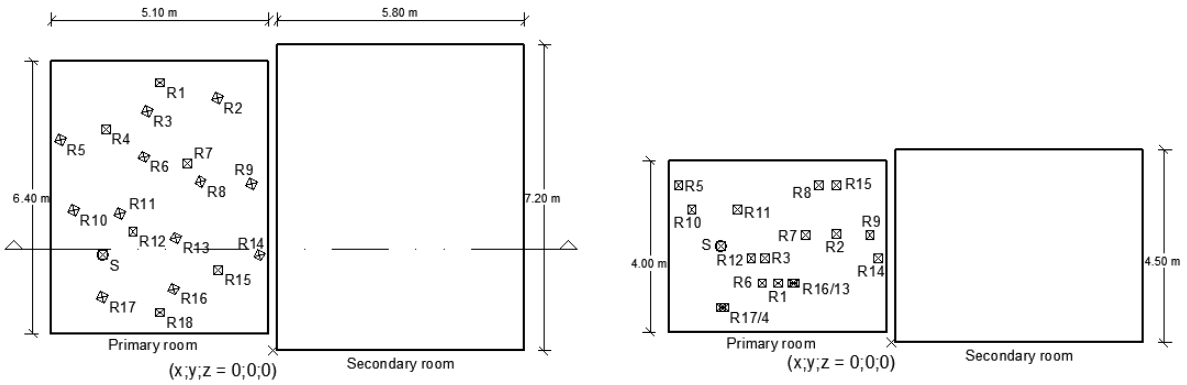

Figure 2 –Floor plan (left) and vertical cross-section (right) of the room system used in the computational model (without coupling) with source and receiver positions.

The domain consists of a volume of air with characteristics that follow the ideal gas law. The domain is spatially discretised in unstructured tetrahedral elements with a minimum of 6 element per wavelength in order to produce meaningful results (20,21). Two adjacent elements have a maximum volume growth ratio of 1.5. Temporal discretisation is expressed relative to the spatial discretisation. Since temporal discretisation has a higher influence on the error in the results (20,22), the number of temporal nodes per wave period is larger than the number of spatial nodes per wavelength. A CFL condition of 0.2 is maintained, meaning that the minimum number of temporal nodes per wavelength (time step) is 5 times as large as the number of spatial nodes per wavelength.

An impulse response is recorded on 18 receiver positions spread over the primary room. The locations of the positions are shown in figure 2.

3.2 Validation study

The FEM computational model is validated using impulse response measurement data of a similar system of coupled volume rooms found at the acoustics laboratory of the Eindhoven University of Technology. The simulated decay curve heavily relies on the assumed boundary properties of the laboratory room system. For this reason, the validation focuses on the frequency content of the measured and simulated decay curves. Figure 3 shows the measurement and simulation results for the 63 Hz and 125 Hz octave bands, both corrected for source power spectrum. From the graph it can be observed, that at 46 Hz the simulation shows a drop in level that is not present in the measurements. At 150 Hz the simulation shows a much higher level than the measurement. Also at 100 Hz the simulation shows a peak in level that is not present in the measurement. The cause of these anomalies is unclear. However, overall the simulations show a good agreement with the measurements.

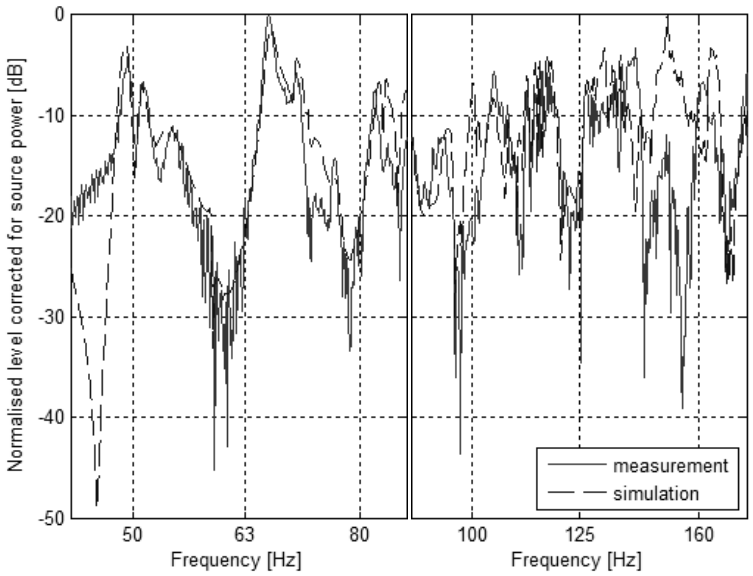

Figure 3 – Source power corrected simulation and measurement results for the two simulations of respectively the 63 Hz, and 125 Hz full octave band.

4. RESULT AND DISCUSSION

4.1 Influence of receiver location

The acoustic pressure in the time-domain simulations is recorded at 18 positions in the primary room. For the 63 Hz 1/3 octave band, the 90 dB decay time of all configurations is shown in figure 4. The 90 dB decay time fluctuates over the positions within each configuration, but there is no strong fluctuation over the configurations. This indicates that the difference in the decay curves for different positions is mainly due to the geometry and corresponding modal shapes in the primary room instead of the aperture distribution and location.

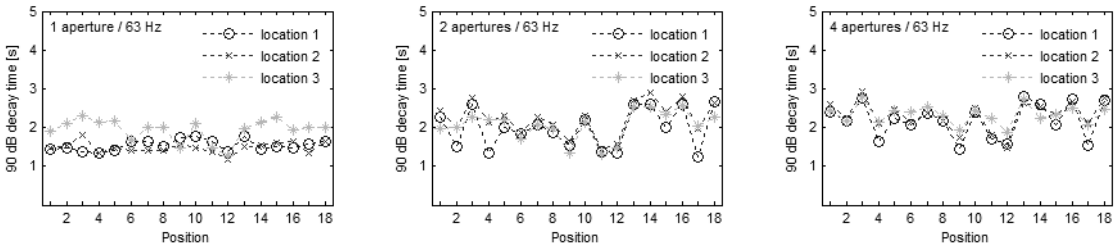

Figure 4 – Computed 90 dB decay time for 18 receiver positions of each configuration to show the influence of receiver location on the decay curve in relation to aperture location and distribution.

4.2 Frequency dependence

The results of the time-domain simulations for each configuration are filtered in 1/3 octave bands. In figure 5 the computed decay ratio, ΔdB and 90 dB decay time, averaged over the receiver positions for each configuration, are shown per 1/3 octave band. The decay curves vary strongly over the evaluated frequency bands. No relation has been found between the centre frequency of the considered band and the level or rate of the decay. This is in contrast with the expectations from the reduced acoustic transparency of apertures at low frequencies.

In order to show whether the acoustic transparency of the apertures does significantly change in the frequency range of interest, the normalised power output of the combinations of apertures is approximated. To do so the apertures are represented by a piston in a plane boundary computed with equation 1. The results in figure 6 show that the radiated power increases with increasing frequency and approaches a limiting value that is reached between 200 Hz and 500 Hz dependent on the aperture distribution. Within the frequency range of interest (the 31.5 Hz, 63 Hz and 125 Hz full octave bands) the acoustic transparency thus increases with increasing frequency. With regard to the optimal range for an aperture opening of 0.5% to 1.5%, an aperture with reduced acoustic transparency effectively equals an aperture with a smaller surface area. The result is that the energy feedback from the secondary room happens at a lower rate. Therefore, the level in the late decay is expected to be lower.

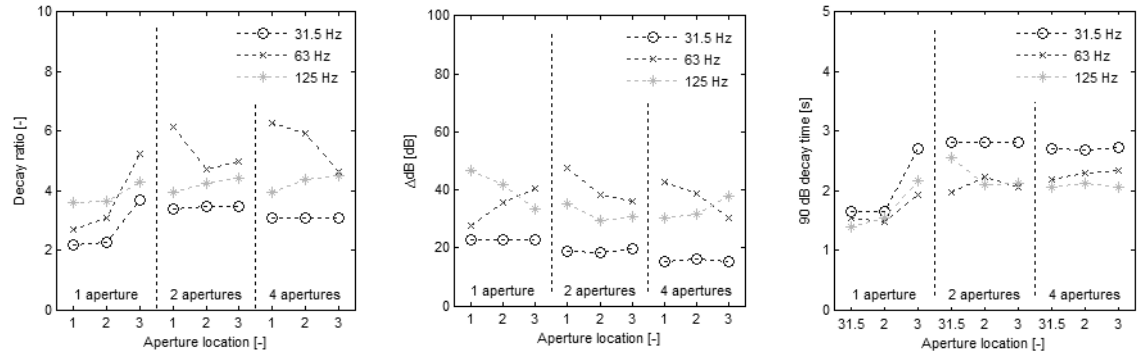

Figure 5 – Computed decay ratio, ΔdB and 90 dB decay time, averaged over the receiver positions for each configuration, arranged to show the dependency on frequency.

In order to give an indication whether the acoustic transparency of the apertures might have a systematic effect on the decay curve in the current results, the decay curves are compared to a decay curve obtained from the statistical acoustics model for coupled volume rooms given in section 2.2. The statistical acoustics model assumes full transparency of the apertures. This would mean that the early decay is at a slightly faster rate, because more energy is transferred to the secondary room. The late decay should be at a higher level since the more transparent aperture allows a higher intensity of energy feedback.

In the time-domain simulation results in figure 6, the initial decay is in all configurations less or equally steep as the statistical acoustics results. This indicates a less transparent opening (i.e. less energy is transferred to the secondary room). The level of the late decay is lower in most configurations and slightly higher in some configurations. Figure 6 thus shows an indication that for low frequencies, the apertures are less transparent and lead to a frequency dependent coupling effect.

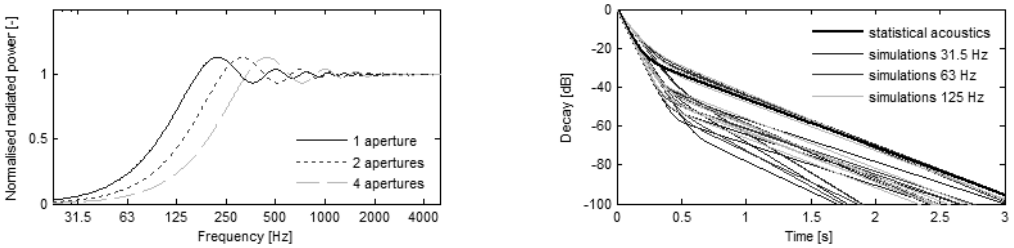

Figure 6 – Aperture transparency approximated as normalized radiated power of a piston in a plane boundary (left) and time domain simulation results compared to statistical acoustics results (right).

4.3 Aperture location

For each number of apertures, 3 variants are modelled with different aperture location. The decay ratio, ΔdB and 90 dB decay time, averaged over the receiver positions for each configuration are shown in figure 7. A systematic effect of changing the aperture location can be observed.

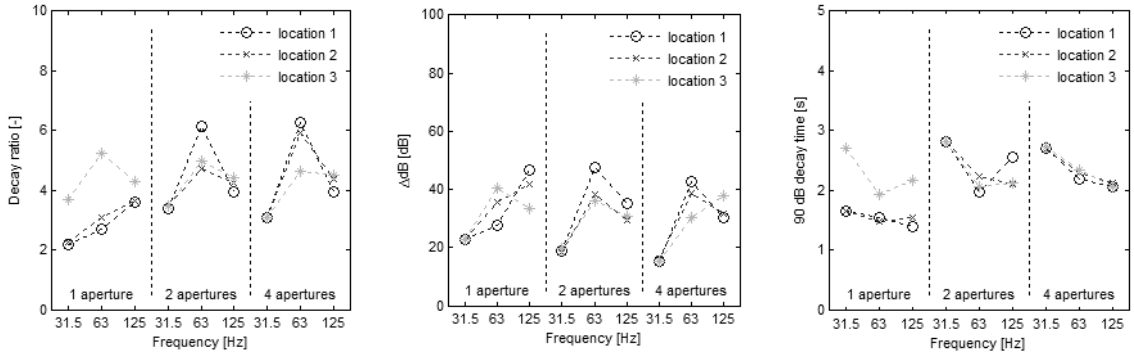

Figure 7 – Computed decay ratio, ΔdB and 90 dB decay time, averaged over the receiver positions for each configuration, arranged to show the influence of aperture location.

The effect is most clear when looking at the decay ratio and 90 dB decay time, meaning that the variation is in the level of the late decay. This indicates that on certain locations the feedback of energy from the secondary room occurs at a higher rate. An eigenfrequency analysis is performed to verify whether this coincides with the modal shapes in the secondary room. The analysis focuses on the magnitude of the sound intensity on the surface of the apertures as a result from the modal shapes (so without the presence of a source and apertures). The sound intensity magnitude is integrated over the surface to obtain the sound power magnitude, a single number quantity for the total feedback to the primary room. This is compared to the 90 dB decay time of the configurations and shown in figure 8. The graphs show a strong correlation between the 90 dB decay time and sound power magnitude on the aperture surface in the secondary room, mainly for the 1 and 4 aperture configurations. It shows that the level of the late decay from the time-domain simulations is strongly influenced by the modal shapes in the secondary room. When the aperture is located in a region with a high surface intensity magnitude, the level of the late decay from the time-domain simulations is high as well. For the 2 aperture configurations, the correlation is less strong. This is mainly due to the large influence of the aperture location on the modal shapes in the secondary room at some frequencies. Since only the secondary room is modelled, there are no apertures and these effects are not taken into account in the incident sound power derived from the modal analysis.

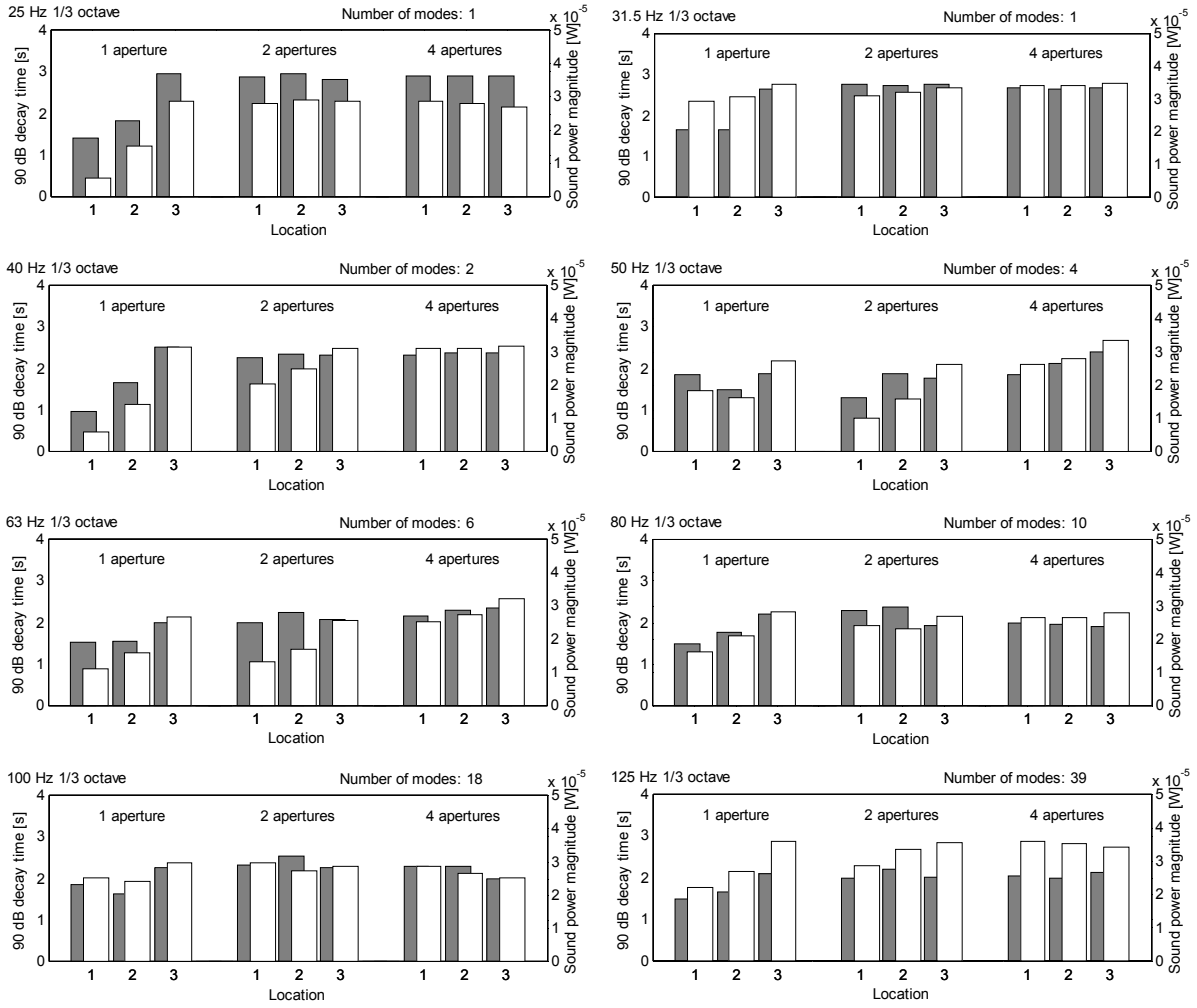

Figure 8 - Computed 90 dB decay time (grey) and sound power magnitude (white) for the decay curves of each configuration per1/3 octave band.

4.4 Aperture distribution

In section 4.2, the acoustic transparency of different sized apertures is approximated, showing that a single large aperture is acoustically more transparent than a set of smaller apertures with an equal total surface area. Therefore, it would be expected that the level of the late decay in the single aperture configuration is higher than in the 2 and 4 aperture configurations. Figure 9 shows the decay ratio, ΔdB and 90 dB decay time, averaged over the receiver position per 1/3 octave band for varying aperture distributions.

In contrary to the expectations, no systematic effect of the number of apertures on the 90 dB decay time, decay ratio or ΔdB is observed. If the aperture distribution has an effect on the decay as would be expected from the radiated power of a piston in a plane boundary, the effect is overruled by other effects. While altering the aperture distribution, also the location of the apertures changes. This might be the cause of the strong variation. Therefore, if the aperture distribution has an effect, this is expected to be more clear for secondary rooms with larger volumes, where the modal behaviour is less strong in the frequency range of interest.

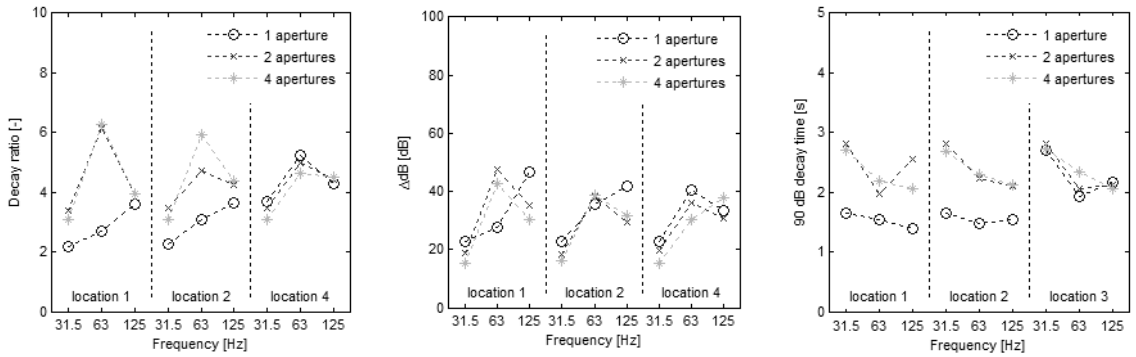

Figure 9 – The computed decay ratio, ΔdB and 90 dB decay time, averaged over the receiver positions for each configuration, arranged to show the influence of aperture distribution.

5. CONCLUSIONS

The sound energy decay in coupled volume rooms is studied for low frequencies. The study shows that the location of the apertures between two rooms has a large influence on the decay curve due to the modal shapes in the secondary room. When the intensity on the aperture surface is high as a result of the model shapes in secondary room, the feedback of energy to the primary room is taking place at a higher rate than when the intensity on the aperture surface is low.

Furthermore, the location of the receiver affects the sound energy decay curve. This effect is independent of the aperture location and distribution, indicating that the variation is property of the primary room, probably the modal shapes.

A systematic frequency dependence has not been found, but is likely to be present due to the reduced aperture transparency at low frequencies. An indication to this extent has been found in the comparison with statistical theory. Similarly, no systematic effect of aperture distribution has been found, but would be expected because a single large aperture is acoustically more transparent than a set of smaller apertures with an equal total surface area. These effects are likely to be more clear for secondary rooms with larger volumes, where the modal behaviour is less strong in the frequency range of interest.

The quantifiers decay ratio and ΔdB, are found to have some limitations. Together, the quantifiers do not uniquely describe a decay curve and without the decay curve itself they fail to enable a clear comparison between late decays with different slope and level. To compare the level of the late decay in this research, the additional quantifier 90 dB decay time is used. A more universally applicable quantifier would be use of the 60 dB decay time.

REFERENCES

1. Sabine WC. Collected Papers of W.C. Sabine. Cambridge: Harvard University Press; 1922.
2. Eyring CF. Reverberation Time in “Dead” Rooms. J Acoust Soc Am. 1930;1(3):217–41.
3. Millington G, Sette WJ. A modified formula for reverberation. J Acoust Soc Am. 1932;(4):69–82.
4. Bradley DT, Wang LM. The effects of simple coupled volume geometry on the objective and subjective results from nonexponential decay. J Acoust Soc Am. 2005;118(3):1480–90.
5. Ermann M. Coupled Volumes: Aperture Size and the Double–Sloped Decay of Concert Halls. Build Acoust. 2005;12:1–14.
6. Valeau V, Billon A, Sakout A, Hodgson M. Prediction of the Acoustics of Coupled Spaces With the Acoustic-Diffusion Model. In: Proceedings of the 9th Western Pacific Acoustics Conference. 2006.
7. Summers JE, Torres RR, Shimizu Y. Statistical-acoustics models of energy decay in systems of coupled rooms and their relation to geometrical acoustics. J Acoust Soc Am. 2004;116(2):958–69.
8. Xiang N, Escolano J, Navarro JM, Jing Y. Investigation of the effect of aperture sizes and receiver positions in coupled rooms. J Acoust Soc Am. 2013;133(6):3975–85.
9. Kuttruff H. Room Acoustics. 5th editon. New York: Taylor & Francis; 2010.
10. Eyring CF. Reverberation time measurements in coupled rooms. J Acoust Soc Am. 1931;3(2):181–206.
11. Ermann M. Five sensitivities of a coupled volume concert hall: a compendium. 2006.

12. Bradley DT, Wang LM. Optimum absorption and aperture parameters for realistic coupled volume spaces determined from computational analysis and subjective testing results. J Acoust Soc Am. 2010;127(1):223–32.
13. Smith PW. Statistical models of coupled dynamical systems and the transition from weak to strong coupling. J Acoust Soc Am. 1979;65(3):695–8.
14. Bradley DT, Wang LM. Quantifying the Double Slope Effect in Coupled Volume Room Systems. Build Acoust. 2009;16(2):105–23.
15. Xiang N, Goggans PM, Jasa T, Kleiner M. Evaluation of decay times in coupled spaces: reliability analysis of Bayeisan decay time estimation. J Acoust Soc Am. 2005;117(3):3707–15.
16. Schroeder MR, Kuttruff KH. On Frequency Response Curves in Room. Comparison of Experimental, Theoretical, and Monte Carlo Results for the Average Frequency Spacing between Maxima. J Acoust Soc Am. 1962;34(1):76–80.
17. Ermann M, Johnson M. Exposure and materiality of the secondary room and its impact on the impulse response of coupled-volume concert halls. J Sound Vib. 2005;284(6):915–31.
18. Harrison BW, Madaras G. Computer modeling and prediction in the design of coupled volumes for a 1000-seat concert hall at Goshen College, Indiana. J Acoust Soc Am. 2001;109(5):2388–2388.
19. Xiang N, Robinson P, Botts J. Comment on “Optimum absorption and aperture parameters for realistic coupled volume spaces determined from computational analysis and subjective testing results” [J. Acoust. Soc. Am. 127, 223-232 (2010)]. J Acoust Soc Am. 2010;128(11):2539–42.
20. Comsol user guide. COMSOL - The Acoustics Module User’s Guide. In: COMSOL user guide. 4.3 ed. COMSOL; 2013.
21. Marburg S. Six Boundary Elements Per Wavelength: Is That Enough? J Comput Acoust. 2002;10(1):25–51.
22. Knudsen VO, Harris CM. Acoustical Designing in Architecture. American Institute of Physics for the Acoustical Society of America; 1970.